in Table I to the published values for native sulfmyoglobin. Owing to the relative instability of the new sulfmyoglobin derivatives, we estimate that our proteins are 80–90% pure, so that the values listed in Table I are best regarded as lower limits of the true values.

As neither deuteroheme IX or mesoheme IX possesses vinyl substituents, the present results establish that vinyl groups are not required for sulfmyoglobin formation. Nearly 50 years ago, Michel reported that hematoheme-substituted myoglobin, another derivative ostensibly devoid of heme vinyl groups, can also form sulfmyoglobin.[13] However, as hematoheme is now known to contain contaminants of vinyl-containing species, the present findings eliminate this source of ambiguity and are consistent with resonance Raman results for native sulfmyoglobin that suggest the presence of both vinyl substituents.[14,15]

Our finding that the heme-substituted sulfmyoglobin derivatives are initially obtained as a mixture of Fe(II) and Fe(III) species (i.e., that they are more readily autoxidized than native sulfmyoglobin) suggests that the reduction potentials of deuterosulfmyoglobin and mesosulfmyoglobin are significantly lower than the reduction potential of native sulfmyoglobin. As the reduction potentials of mesohememyoglobin and deuterohememyoglobin are reported to be only 6–22 mV lower than that of native myoglobin,[16] it may be that the magnitude of heme-substituent effects on the reduction potentials of sulfheme proteins is significantly different from the corresponding effects on the native heme prosthetic group.

In addition to the insight that this work provides into the involvement of heme vinyl groups in sulfmyoglobin formation, it is our expectation that the new sulfmyoglobin derivatives described here should be of use in subsequent NMR and resonance Raman studies and should help to facilitate rigorous structural characterization of the sulfheme prosthetic group.

Addendum

While this paper was being reviewed, a related report appeared that reached conclusions consistent with those reported here.[17]

Acknowledgment. This work was supported by Grant MA-7182 from the Medical Research Council of Canada and was performed in collaboration with Thomas M. Loehr and Laura A. Andersson of the Oregon Graduate Center, whose work on this subject is supported by Grant GM-34468 from the National Institutes of Health.

Registry No. Heme, 14875-96-8.

---

(13) Michel, H. O. *J. Biol. Chem.* **1938**, *126*, 323–348.
(14) Andersson, L. A.; Loehr, T. M.; Lim, A. R.; Mauk, A. G. *J. Biol. Chem.* **1984**, *259*, 15340–15349.
(15) Andersson, L. A.; Loehr, T. M.; Chang, C. K.; Mauk, A. G. *J. Am. Chem. Soc.* **1985**, *107*, 182–191.
(16) Brunori, M.; Saggese, U.; Rotilio, G. C.; Antonini, E.; Wyman, J. *Biochemistry* **1971**, *10*, 1604–1609.
(17) Chatfield, M. J.; La Mar, G. N.; Balch, A. L.; Smith, K. M.; Parish, D. W.; Le Page, T. J. *FEBS Lett.* **1986**, *206*, 343–346.

Contribution from the Department of Applied Chemistry,
Faculty of Engineering, Tohoku University, Sendai 980, Japan

Anion-Exchanged Hydrotalcite-like-Clay-Modified Electrodes

Kingo Itaya,* Hsien-Chang Chang, and Isamu Uchida

Received July 11, 1986

There has been considerable interest in modified electrodes using inorganic layers such as clay,[1-4] zeolite,[5] and transition-metal cyanides.[6] Modification of electrodes with a thin layer of clay has been reported by Bard et al.[1] and other groups.[2-4] In addition to the studies of modified electrodes, it has recently been shown that free-standing pillared clay films behave as cation-exchange membranes by measurements of the membrane potential.[1e] The clay colloid used in the previous works[1-4] was sodium montmorillonite, one of the members in the smectic group of clays.[7] Montmorillonite has an expanding 2:1 layer lattice structure and has a cation-exchange capacity due to unbalanced charges in the interior of the layers.[7] Cations such as $Ru(bpy)_3^{2+}$ (bpy = 2,2′-bipyridine), $Fe(bpy)_3^{2+}$, $Os(bpy)_3^{2+}$, or MV^{2+} (methylviologen) incorporated by the cation-exchange reaction into montmorillonite films were found to be electroactive.[1-4]

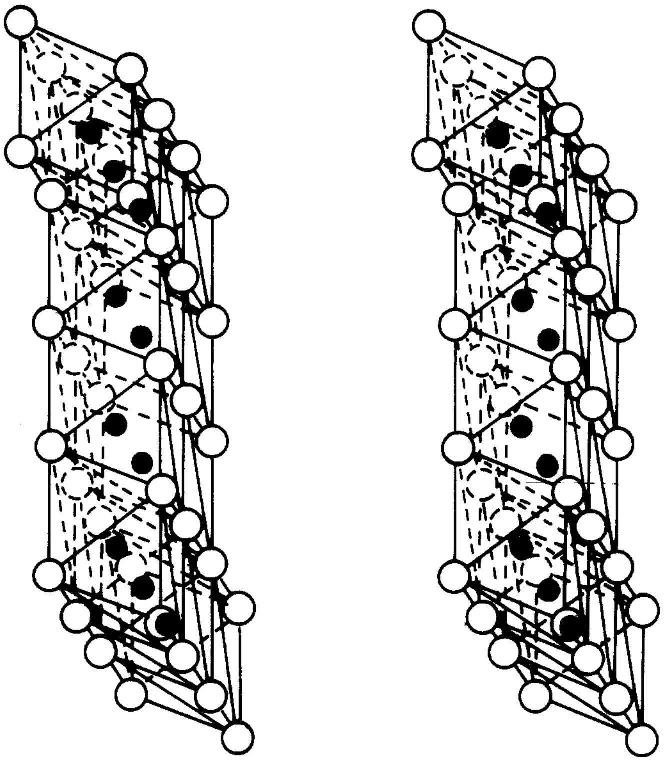

Figure 1. Perspective structure of positively charged brucite-like layers. Anions located in the interlayer are omitted for the sake of clarity: (○) hydroxyl; (●) Al^{3+} or Mg^{2+}.

On the other hand, it is well-known that the rhombohedral hydrotalcite $Mg_6Al_2(OH)_{16}CO_3{\cdot}4H_2O$ consists of positively charged brucite-like layers $[Mg_6Al_2(OH)_{16}]^{2+}$ and negatively charged interlayers $[CO_3{\cdot}4H_2O]^{2-}$, as shown in Figure 1.[7-9] A series of synthetic hydrotalcite-like compounds (HT) has been prepared by reactions of NaOH with mixed Mg–Al solutions.[9,10] It was reported that anions such as Cl^-, NO_3^-, or SO_4^{2-} located in the interlayer of HT would be substituted with other anions by anion-exchange reactions.[9d,11]

On the basis of the above background, we report in this paper a new type of clay-modified electrodes using HT, demonstrating

---

(1) (a) Ghosh, P. K.; Bard, A. J. *J. Am. Chem. Soc.* **1983**, *105*, 5691. (b) Ghosh, P. K.; Mau, A-W. H.; Bard, A. J. *J. Electroanal. Chem. Interfacial Electrochem.* **1984**, *169*, 315. (c) Ege, D.; Ghosh, P. K.; White, J. R.; Equey, J. F.; Bard, A. J. *J. Am. Chem. Soc.* **1985**, *107*, 5644. (d) White, J. R.; Bard, A. J. *J. Electroanal. Chem. Interfacial Electrochem.* **1986**, *197*, 233. (e) Itaya, K.; Bard, A. J. *J. Phys. Chem.* **1985**, *89*, 5565.
(2) Yamagishi, A.; Aramata, A. *J. Chem. Soc., Chem. Commun.* **1984**, 119.
(3) Liu, H. Y.; Anson, F. C. *J. Electroanal. Chem. Interfacial Electrochem.* **1985**, *184*, 411.
(4) Kamat, P. V. *J. Electroanal. Chem. Interfacial Electrochem.* **1984**, *163*, 389.
(5) Murray, C. G.; Nowak, R. J.; Rolison, D. R. *J. Electroanal. Chem. Interfacial Electrochem.* **1984**, *164*, 205.
(6) Itaya, K.; Uchida, I.; Neff, V. D. *Acc. Chem. Res.* **1986**, *19*, 162.
(7) Van Olphen, H. *An Introduction to Clay Colloid Chemistry*; Wiley: New York, 1977.
(8) Frondel, C. *Am. Mineral.* **1941**, *26*, 295.
(9) (a) Miyata, S. *Clays Clay Miner.* **1975**, *23*, 369. (b) Miyata, S.; Okada, A. *Clays Clay Miner.* **1977**, *25*, 14. (c) Miyata, S.; Hirose, T. *Clays Clay Miner.* **1978**, *26*, 441. (d) Miyata, S. *Clays Clay Miner.* **1983**, *31*, 305.
(10) (a) Brindley, G. W.; Kikkawa, S. *Clays Clay Miner.* **1981**, *28*, 87. (b) Kikkawa, S.; Koizumi, M. *Mater. Res. Bull.* **1982**, *17*, 191.
(11) Ikeda, T.; Amoh, H.; Tasunaga, T. *J. Am. Chem. Soc.* **1984**, *106*, 5772.

0020-1669/87/1326-0624$01.50/0

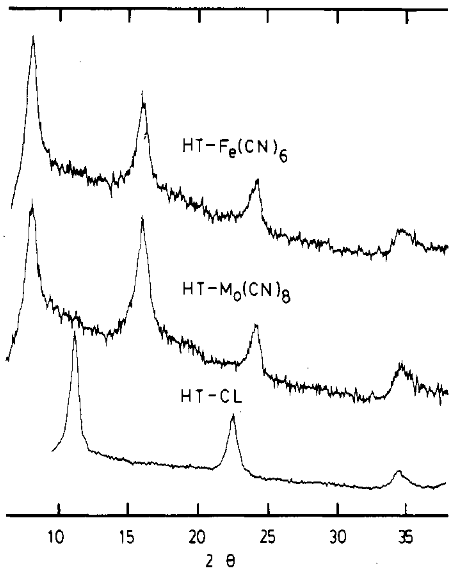

Figure 2. X-ray powder diffractions for HT–Cl, HT–$Mo(CN)_8$, and HT–$Fe(CN)_6$.

that anionic redox species incorporated into its films are electrochemically active.

Experimental Section

Chemicals. Three different types of HT were kindly supplied by Kyowa Chemical Co., having the anions of Cl^- (HT–Cl), NO_3^- (HT–NO_3), and CO_3^{2-} (HT–CO_3) in the interlayer. The anion-exchange properties of these samples have already been reported by Miyata.[9d] The ion-exchange capacity of HT–Cl was about 1.4 mmol g^{-1} of univalent ion. $K_4Mo(CN)_8 \cdot 2H_2O$ was prepared according to a literature procedure.[12] K_2IrCl_6 and $K_3Fe(CN)_6$ were obtained commercially.[13] All other chemicals used were reagent grade.

Procedure. The powder samples for the X-ray analysis were prepared as follows: Each HT (1 mequiv) and an excess amount (more than 5 mequiv) of 20 mM aqueous solutions of the above redox anions were placed in a flask and stirred for 24 h. The contents of the flask were subsequently purified by repeated cycles of centrifugation using distilled water and then air-dried at room temperature. X-ray diffraction data were obtained by using a nickel filter with a diffractometer (Rigaku Denki). The Cu anode was operated at 30 kV and 10 mA.

Films of HT–Cl for electrochemical studies were prepared on SnO_2 plates. Two grams of HT–Cl was dispersed in 100 mL of distilled water or ethanol by ultrasonication for 1 h. The dispersed HT–Cl was then centrifuged at 2000 rpm for 1 h, and the white precipitate was discarded. The supernatants were used for film preparation. Films were cast by placing a measured volume (10–50 μL) of the clay dispersions on SnO_2 plates and allowing the solvent to evaporate at room temperature for a few hours. A typical thickness of the films was ca. 100 nm, as estimated by the observed interference color, as described in a previous paper.[1e] $Mo(CN)_8^{4-}$, $Fe(CN)_6^{3-}$, and $IrCl_6^{2-}$ were incorporated into the film by soaking the electrodes in 20 mM aqueous solutions of these ions for ca. 1 h. After this ion-exchange reaction, the electrodes were washed several times with distilled water and then used for the electrochemical experiments in 0.1 M Na_2SO_4 (pH 6.0). Electrochemical measurements were done with a Solartron Model 1286 potentiostat. A saturated calomel electrode (SCE) was employed as a reference electrode.

Results and Discussion

X-ray Powder Diffraction of HT. The three anion-exchanged hydrotalcite-like compounds prepared above are abbreviated as HT–$Mo(CN)_8$, HT–$Fe(CN)_6$, and HT–$IrCl_6$, respectively. Figure 2 shows an example of the X-ray powder diffractions of HT–Cl, HT–$Fe(CN)_6$, and HT–$Mo(CN)_8$. The last two samples were prepared by the ion-exchange reaction using HT–Cl, as described above. The first two sharp peaks observed at about 11 and 22° for the HT–Cl sample have been assigned by the Miller indices of (003) and (006), respectively. The peak at ca. 34.5° is composed of diffractions from (100), (102), and (009). These features in the X-ray diffraction pattern are well in accord with the results reported in the literature.[9a] The diffractions for HT–$Mo(CN)_8$ and HT–$Fe(CN)_6$, however, showed four main peaks in the range of angle observed. The first three peaks can be assigned to (003), (006), and (009), respectively, and the last peak, which appeared at 34.4°, assigned to (100) and (102). The shift of (003), (006), and (009) to lower scattering angles indicates straightforwardly that the thickness of the unit layer (d_{003}) increases with the incorporation of these anions. The same experiment was carried out for the sample of HT–$IrCl_6$ prepared from HT–Cl.

Table I. X-ray Diffraction Data

sample	basal spacing,[a] Å	interlayer sepn,[b] Å
HT–Cl	8.0	3.23
HT–$Mo(CN)_8$	11.2	6.43
HT–$Fe(CN)_6$	11.2	6.43
HT–$IrCl_6$	10.8	6.03

[a] The distance (d_{003}) between the adjacent two layers. [b] The thickness of the brucite layer is 4.77 Å.

Table I summarizes the results obtained from the X-ray diffraction data. The interlayer separation is calculated by subtracting the thickness of the brucite layer (4.77 Å) from that of the unit layer (d_{003}).[9a] The compound HT–$Fe(CN)_6^{4-}$ (ferrocyanide) was directly synthesized, by a coprecipitation method, in the presence of potassium ferrocyanide.[9c,10b] The literature value (11.2 Å) of the unit layer[9c] is almost identical with the present one, indicating that the interlayer separations are almost the same for both HT–$Fe(CN)_6^{3-}$ and HT–$Fe(CN)_6^{4-}$. It was proposed previously for the orientation of the $Fe(CN)_6^{4-}$ ion that its symmetric C_3 axis was perpendicular to the layer, on the basis of the observed separation of the interlayer.[10b] The orientation of $Fe(CN)_6^{3-}$ seems to be identical with that of $Fe(CN)_6^{4-}$ because the same interlayer separation was found for both $Fe(CN)_6^{3-}$ and $Fe(CN)_6^{4-}$. We also examined the X-ray study using samples dried at room temperature under a vacuum and found the same values for the interlayer separations. This suggests that the anions are relatively strongly bound into the interlayer region of HT. The above results can be compared with a sodium montmorillonite film, where the basal spacings are very dependent upon the water-vapor pressure in the atmosphere.[1e,7]

A similar result was obtained by using HT–NO_3, instead of HT–Cl. However, we found that the HT–CO_3 sample did not show any evidence for an anion-exchange reaction with the redox anions examined here, even though higher concentrations (saturated) of the redox anions were employed for the anion-exchange reaction. Since the CO_3^{2-} anion is strongly bound in the interlayer of hydrotalcite-like compounds,[9d] the exchange reaction does not proceed under the present conditions. For this reason, further electrochemical studies were carried out by using the HT–Cl sample.

Electrochemistry of the Incorporated Anions. Figure 3A shows current–potential curves obtained in 0.1 M Na_2SO_4 with a HT–$Mo(CN)_8$-modified SnO_2 electrode under successive potential cycling. The peak currents for the $Mo(CN)_8^{4-/3-}$ couple incorporated in the interlayer are clearly observed at ca. 0.5 V vs. SCE, which is almost in complete accord with the half-wave potential of this couple in the same solution.[14] Although the peak currents decrease during initial potential scans as shown in Figure 3A, a steady voltammogram is obtained after about 10–20 repeated cycles. The steady voltammogram did not show a further decrease after 60-min cycling, indicating that the $Mo(CN)_8^{4-/3-}$ couple is fairly strongly incorporated into the interlayer region of HT. The initial decrease in the peak current might be due to the attainment of an exchange equilibrium between $Mo(CN)_8^{4-}$ and SO_4^{2-} or a loss of poorly adhered HT layers during the potential scan. A similar result was also observed in a 0.1 M KCl solution.

The change in the cyclic voltammetric behavior as a function of sweep rate was examined as shown in Figure 3B. Table II shows

---

[12] Furman, N. H.; Miller, C. O. *Inorg. Synth.* **1950**, *3*, 160.

[13] Itaya, K.; Uchida, I.; Toshima, S. *J. Phys. Chem.* **1983**, *87*, 105.

[14] Saji, T.; Maruyama, Y.; Aoyagi, S. *J. Electroanal. Chem. Interfacial Electrochem.* **1978**, *86*, 219.

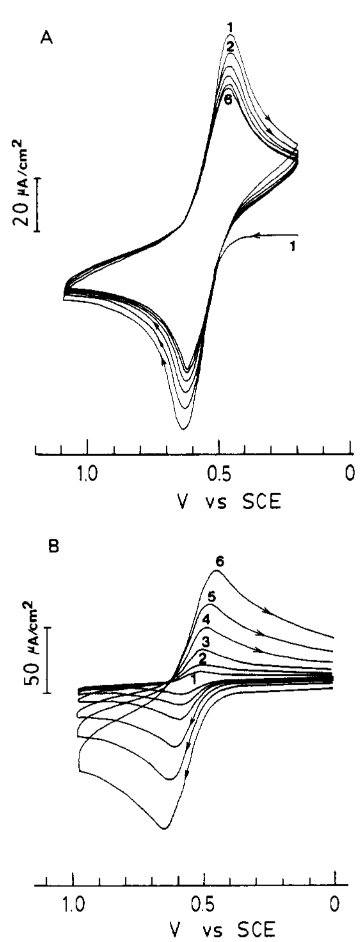

Figure 3. Cyclic voltammograms of $Mo(CN)_8^{4-}$-incorporated HT-modified SnO_2 electrodes in 0.1 M Na_2SO_4: (A) voltammograms obtained under successive potential cycling, the number in the figure showing the repeated cycle between 0.2 and 1.1 V at a scan rate of 50 mV s^{-1}; (B) steady voltammograms, with scan rates of 5 (1), 10 (2), 20 (3), 50 (4), 100 (5), an 200 (6) mV s^{-1}.

Table II. Cyclic Voltammetric Data for a HT–$Mo(CN)_8$-Modified Electrode[a]

	v, mV s^{-1}					
	5	10	20	50	100	200
i_{pa}, μ_A cm^{-2}	11	19	30	50	74	106
ΔE_p, mV	60	60	80	120	150	200

[a] 3 × 10^{-9} mol cm^{-2} of $Mo(CN)_8^{4-}$ contained in film ca. 100 nm thick on an SnO_2 electrode.

actual data for the anodic peak currents (i_{pa}) and for the difference between anodic and cathodic peak potentials (ΔE_p) observed at the different scan rates. The peak current was approximately proportional to the scan rate (v) up to 10 mV s^{-1} and then proportional to $v^{1/2}$ at sweep rates greater than 20 mV s^{-1}. Note that the difference of the peak potentials (ΔE_p) was increased from 60 mV, which was observed at 5 and 10 mV s^{-1}, with increasing scan rate, as shown in Table II. This observation suggests that the rate of the heterogeneous electron-transfer reaction is slow or the film of HT is highly resistive. A similar result has been reported for montmorillonite-modified electrodes.[1c]

However, the peak current in the diffusion-controlled region (50–200 mV s^{-1}) was used to estimate a diffusion coefficient for $Mo(CN)_8^{4-}$ incorporated into HT, yielding 8 × 10^{-12} cm^2 s^{-1}. The total number of moles of $Mo(CN)_8^{4-}$ was measured by integrating the area under the oxidation peak at 5 mV s^{-1} (3 × 10^{-9} mol). The thickness of the film was about 100 nm. It is noteworthy that the values obtained here seem to be still rather qualitative and depend primarily on an accuracy in measurements of the film thickness. It was found that the surface of the HT layer on electrodes showed a rough structure observed under a scanning electron micrograph. In order to decrease the film thickness to less than 100 nm, we applied a more dilute solution of HT–Cl to the electrode surface. However, the HT–Cl colloids coagulated on the surface of the SnO_2 electrode, resulting in an island structure of the film. A further improvement for the film preparation is eventually necessary for the measurement of accurate diffusion coefficients. The crystal size of the sample of HT–Cl examined here was estimated as ca. 100 nm by the half-maximum breadth of X-ray diffractions.[15] It might be possible to prepare a smooth coating when smaller particles of HT–Cl are employed.

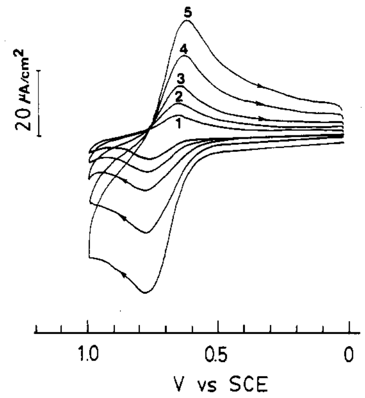

Figure 4. Steady voltammograms of $Fe(CN)_6^{3-}$-incorporated HT-modified SnO_2 electrodes in 0.1 M Na_2SO_4. Scan rates: 5 (1), 10 (2), 20 (3), 50 (4), 100 (5) mV s^{-1}.

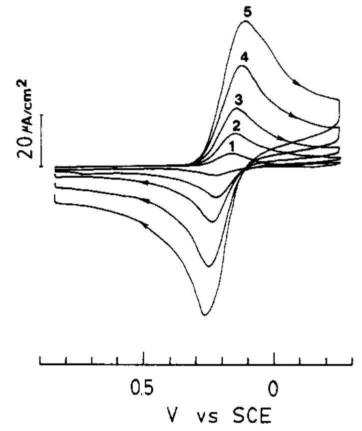

Figure 5. Steady voltammograms of $IrCl_6^{2-}$-incorporated HT-modified SnO_2 electrodes in 0.1 M Na_2SO_4. The initial potential was held at 0 V. Scan rates: 5 (1), 10 (2), 20 (3), 50 (4), 100 (5) mV s^{-1}.

Figures 4 and 5 show steady voltammograms for HT–$Fe(CN)_6$- and HT–$IrCl_6$-modified electrodes, respectively. For HT–$IrCl_6$, the voltammograms were recorded after the initial potential was held at 0 V vs. SCE for 10 s. Therefore, all $IrCl_6^{2-}$ ions incorporated into the film were reduced to the form of $IrCl_6^{3-}$ at 0 V. The peak potentials for the $Fe(CN)_6^{3-/4-}$ and $IrCl_6^{2-/3-}$ couples were near those obtained for these solution species at a bare SnO_2 electrode.

The changes in the cyclic voltammetric behavior as a function of sweep rate were almost the same as that for HT–$Mo(CN)_8$ as shown in Figure 3B. This indicates that the diffusion coefficients of the $Fe(CN)_6^{3-/4-}$ and $IrCl_6^{2-/3-}$ couples in the film seem to be of the same order of magnitude for that of the $Mo(CN)_8^{3-/4-}$ couple. The stability of the voltammograms in Figures 4 and 5 is also excellent.

In conclusion, the HT film has a potential application for a new clay-modified electrode, because of its anion-exchange properties.

Acknowledgment. We thank Dr. S. Miyata (Kyowa Chemical Co.) for the supply of hydrotalcite-like compounds. This work was supported by a Grant-in-Aid (61550693) for Scientific Research of the Ministry of Education, Science and Culture, Japan.

---

(15) Miyata, S. *Clays Clay Miner.* **1980**, *28*, 50.